Electrodynamic deorbiting of LEO satellites (*)

M. DOBROWOLNY, G. VANNARONI and F. DE VENUTO
Istituto di Fisica Spazio Interplanetario, CNR - Roma, Italy

(ricevuto il 22 Settembre 1999; revisionato il 27 Dicembre 1999; approvato il 17 Gennaio 2000)

Summary. — In this paper we present realistic calculations of deorbiting times for a LEO satellite through the use of electrodynamic tethers. We refer to two possible tether systems (a bare and a conducting insulated tether) both equipped with an inflatable conducting balloon at the upper end. The calculations take into account average ionospheric properties and the electrical interaction of the wire with the ionosphere. Furthermore, they have been done for several inclination orbits and include also the deviation of the tether from the vertical direction under the combined action of the gravity gradient and the electrodynamic forces. The results obtained for the decay times, for typical constellation satellite, indicate that such tether systems are definitely of interest for the deorbiting application.

PACS 94.20 – Physics of the ionosphere.
PACS 96.50 – Interplanetary space.

1. – Introduction

The accumulation of orbital debris in low earth orbits (between 500 and 2000 km in altitude) in the long run (say, 50 to 100 years from now) will create unacceptable risks to space activities, not only because of collisions with active spacecraft, but also because of the creation of secondary debris which generate a cascade process and determine an exponential increase of the debris population [1].

Conducting tethers have been proposed as a means to deorbit LEO spacecraft [2]. The tether would be deployed upwards from the satellite or object one wants to deorbit and the electrodynamic drag associated with the natural current in the tether would cause orbital decay. A demonstration project, called ProSEDS (Propulsive Small Expendable Deployer System) [3], will be launched by NASA in the year 2000. In this case the tether would be deployed from the upper stage of a Delta rocket and should lead to de-orbiting of the Delta stage, initially put in a 400 km circular orbit, in a time of about 15 days (according to the estimates of the proposers), which has to be compared with the time (about 4 months) a natural orbit decay would take.

It is quite important to evaluate, with realistic models taking into account both the ionospheric environment and the tether equivalent electric circuit, the time it takes to

(*) The authors of this paper have agreed to not receive the proofs for correction.

deorbit a spacecraft, in a given LEO orbit, from its original altitude down to altitudes ($\sim$ 200 km) where atmospheric drag alone causes a rapid re-entry into the Earth's atmosphere. Such an evaluation is important from two points of view. The first, which is obvious, is that the product of the decay time of the tethered system with its cross-section must be smaller than the same product for the satellite alone (involving therefore its natural decay time). The second point of view is that, for the system tether and satellite to work, the deorbiting time must be smaller with respect to the typical time for an impact on the tether of a debris (either natural or artificial) which could break the tether and therefore destroy the deorbiting system (causing, in addition, the production of large debris in the ionosphere).

This second point has in fact been considered very recently [4] by evaluating the impact rates of debris of various sizes on tethers of different dimensions. The conclusions of this paper can be summarized by saying that, with reference to typical times for deorbiting such as the ones obtained in this paper (at least of a few months for typical constellation satellites), single strand tethers of small cross-section in LEO orbits could probably be severed by orbital debris and different tether designs (for example a ribbon type or a multistrand tether like the Hoytether^{TM} [5]), will finally have to be considered for a safe application. Nevertheless, to get an idea of the deorbiting time (which depends on the current in the tether), we can (and we will in this paper) still refer to a simple cylindrical wire for which the calculations are feasible. A ribbon-type tether, of the same length as the wire tethers considered here, is likely to allow even higher currents (and hence better performance), and, at the same time, due to the increase in transverse dimensions, lowers the impact probability with orbital debris to acceptable values.

Recently [6], we have undertaken a comparative evaluation of the merits of three different tether configurations: the insulated tether with a conducting balloon (ITB), a bare tether with a conducting balloon (BTB) and a bare tether only (BTO). The results obtained are pointing out to the importance of using a conducting balloon at the upper tether termination. For given tether and balloon dimensions, the best performance is obtained with the BTB and ITB configurations (in the order), whereas the configuration BTO leads to quite longer deorbiting times.

This study, being devoted to a comparison between the three configurations, was done referring to the simplest case of an equatorial orbit and a straight tether aligned with the vertical direction. As for the ionospheric parameters, orbital velocity, magnetic field and electron temperature were given constant values and only the variation of density with altitude was considered. Because of these simplifications, the numbers obtained for the decay times, although meaningful for the purpose of comparing the three different configurations, must not be considered individually as realistic values.

In this same work [6] we found an analytical approximation (which we checked against a numerical treatment), which considerably simplifies the problem. The simplification consists in the fact that the electrodynamic drag can be obtained analytically as a function of the potential Φ_b at the upper tether termination and all is left is the determination of this potential Φ_b (upon varying ionospheric parameters) through a simple algebraic equation.

The use of this same approximation allows us now to generalize the calculation removing the simplifying assumptions mentioned above. This is what we have done in this paper where we include the altitude variation of orbital velocity and magnetic field, take into account a deviation of the tether from the vertical direction, caused by the

electrodynamic force, and, finally, perform calculations for different orbital inclinations.

The paper is organized as follows. In sect. **2**, referring to circular orbits, we describe the spacecraft orbit in a geomagnetic reference frame. Using this, we derive, in sect. **3**, the electromotive potential, due to the tether motion across magnetic lines, for a given deviation from the vertical direction and for a given inclination j of the spacecraft orbit with respect to the Earth's equatorial plane. The deviation from the vertical direction is expressed through two angles, called α_{in} and α_{out}, the first of which gives the angular deviation in the orbital plane, while the second is the angular deviation out of the orbital plane.

Section **4** derives, in detail, the electrodynamic force due to the interaction of the tether current with the Earth's magnetic field and gives explicit expressions for the components of this force both in the plane of the orbit and out of this plane. In this same section we derive the electrodynamic drag which is that component of the electrodynamic force which causes the system to decay. Section **5** derives, through a balance between gravity gradient and electrodynamic torques, the equations which determine the equilibrium values of the angles α_{in} and α_{out} which define the deviation of the tether from the vertical direction. Both these equations and the equation for the electrodynamic drag contain the tether current (and, in the case of a bare tether, also that part which is collected along its length).

Section **6** is devoted to the determination of this current. We show that the differential equation governing the distribution of potential along the tether can be reconducted to exactly the same form used in the calculation of ref. [6], the only difference being a redefinition of the coefficients entering this equation. As a consequence, we can follow the approximate method of solution used in that paper. We derive the total current I for both the BTB and the ITB configuration.

Section **7** contains results obtained with the formalism developed. We calculate deorbiting of a satellite of mass 500 kg, from an original altitude of 1300 km down to 200 km, with a tether 5 km long and of radius $r_w = 0.4$ mm with an upper balloon of radius $r_{\text{b}} = 2.5$ m. Deorbiting profiles are obtained both for an equatorial orbit and an orbit at 55° inclination and for both the BTB and the ITB configurations. In each case, we show the profile of orbital decay, the variation with altitude of the drag force and the angles α_{in} and α_{out}. In addition, we have performed specific calculations for two constellation satellites (Global Star and Skybridge) using the appropriate parameters. Section **8** contains a discussion of the results obtained and indications for future studies on such tether systems.

2. – Spacecraft orbit

We approximate the Earth's magnetic field with a magnetic dipole with the axis tilted off from the Earth's spin axis by $\phi = 11.5°$. We ignore, in this analysis, the 436 km offset of the dipole center from the center of the Earth.

It will be convenient, in the following, to perform the calculations in a reference frame that is rotated so that it has its z-axis aligned with the axis of the Earth's magnetic dipole (see fig. 1). In addition, in this reference frame, we choose the x-axis oriented along the intersection of the orbital plane with the plane of the magnetic equator. Then the dipole magnetic field can be written as

$$\mathbf{B} = B_0 \mathbf{b} \tag{1}$$

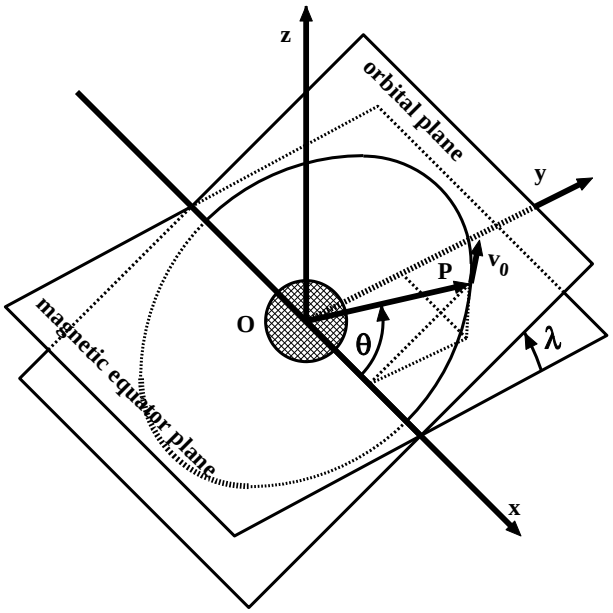

Fig. 1. – Geomagnetic reference frame.

with

$$B_0 = -B_e \frac{R_e^3}{r^3} \tag{2}$$

and

$$\mathbf{b} \equiv \left(\frac{3xz}{r^2}, \frac{3yz}{r^2}, \frac{3z^2}{r^2} - 1 \right). \tag{3}$$

Here $R_e = 6378$ km is the radius of the Earth and $B_e = 0.3$ G is the strength of the magnetic field on the magnetic equator at the surface of the Earth.

We consider a circular orbit, of radius r, with inclination λ with respect to the geomagnetic equator. In the geomagnetic frame previously introduced, we can parametrize the orbit in terms of the orbital anomaly θ which is the angle, with respect to x, swept by the radius vector $\mathbf{r}$, measured starting from the ascending intersection of the orbit with the plane of the magnetic equator. We obtain for the vector $\mathbf{r}$ connecting any given point of the orbit to the center of the Earth (and directed away from the Earth)

$$\mathbf{r} = r \hat{i}_r, \tag{4}$$

where

$$\hat{i}_r \equiv (\cos\theta, \cos\lambda \sin\theta, \sin\lambda \sin\theta) \tag{5}$$

is the unit vector along the local vertical.

In the same parametric representation, the velocity **v** at a given point (directed as the local tangent), will be written as

$$\mathbf{v} = v_0 \hat{i}_v, \tag{6}$$

where

$$\hat{i}_v \equiv (-\sin\theta,\ \cos\lambda\cos\theta,\ \sin\lambda\cos\theta) \tag{7}$$

is the unit vector along the velocity direction and v_0 is the magnitude of the orbital velocity given by

$$v_0 = \sqrt{\frac{GM_e}{r}},$$

where $G = 6.67\cdot10^{-11}\,\mathrm{m^3/kgs^2}$ is Newton's gravitational constant and $M_e = 5.976\cdot10^{24}\,\mathrm{kg}$ is the mass of the Earth. Notice that the plane of the orbit is defined by the unit vectors $\hat{i}_r$ and $\hat{i}_v$.

Using the previous representation for the orbit, we now obtain, for the magnetic field components at any given point along that orbit,

$$\mathbf{b} \equiv (3\sin\lambda\sin\theta\cos\theta,\ 3\sin\lambda\sin^2\theta\cos\lambda,\ 3\sin^2\theta\sin^2\lambda - 1). \tag{8}$$

It is appropriate to recall, at this point, that, due to the tilt of the magnetic dipole with respect to the Earth's equatorial plane, the inclination λ is related to the inclination j of the orbit with respect to the Earth's equatorial plane, by

$$\lambda = j + \phi_0 \sin(\omega_m t),$$

where $\phi_0 = 11.5°$ and $T = 2\pi/\omega_m = 1$ d is the period of the Earth's rotation. λ appears as $\cos\lambda$ or $\sin\lambda$ in our formulation. Expanding (for $\phi_0 \ll \pi/2$), we have, for example

$$\cos\lambda \sim \cos j\left[1 - \frac{1}{2}\phi_0^2\sin^2(\omega_m t)\right] - \phi_0 \sin j \sin(\omega_m t) + O(\phi_0^3).$$

By substituting $\cos\lambda$ with $\cos j$, we make an error which is, at most, of $O(\phi_0 \sin j)$ ($\phi_0 \sim 0.2$ in radians), and a similar reasoning applies to the substitution of $\sin\lambda$ with $\sin j$. As we do not aim at a very precise determination of the deorbiting time, we will take, in the following, $\lambda = j$.

3. – Electromotive potential

The motion of the tether across the geomagnetic field induces an electric field along its length which is given by

$$\mathbf{E} = \mathbf{v} \times \mathbf{B}\ .$$

For an eastward motion of the tether, this electric field is directed upwards so that the upper end of the tether is positive with respect to its lower end. This causes a total induced voltage Φ_{emf} between tether terminations which, for a straight tether, is given by

$$\Phi_{\mathrm{emf}} = \mathbf{E}\cdot\mathbf{L} = (\mathbf{v} \times \mathbf{B})\cdot\mathbf{L}$$

with **L** a vector of magnitude equal to the tether length and directed upwards along the tether.

In studying the electrodynamics of bare tethers, we will have to use the differential form of the induced potential

$$\mathrm{d}\Phi_{\mathrm{emf}} = (\mathbf{v} \times \mathbf{B}) \cdot \mathbf{dl} \tag{9}$$

representing the variation of the emf-induced potential between the points l and $l + \mathrm{d}l$ along the tether length.

The balance between gravity gradient forces and electrodynamic forces, which will be calculated later on, will cause the tether to deviate from the local vertical and, in general, because of nonuniformity of the forces along the tether and because of the fact that the tether is not rigid, the tether orientation will vary along its length, *i.e.* the tether will in fact assume a curved orientation. Although the formulation (9), containing the vector element **dl**, would allow to treat the realistic case of a curved tether shape, in the following analysis we will treat only the simplified case where the tether hangs straight at an angle (to be determined) with respect to the local vertical. In this case the direction of **dl** will not vary along the tether.

Referring to a straight tether, we will however develop our formulation for the general case where the tether is lying out of the orbital plane (the $\hat{i}_r$-$\hat{i}_v$ plane). For this general case we write

$$\mathbf{dl} = \hat{i}_l \, \mathrm{d}l \tag{10}$$

with

$$\hat{i}_l = \cos\alpha_{\mathrm{in}} \cos\alpha_{\mathrm{out}} \hat{i}_r + \sin\alpha_{\mathrm{in}} \cos\alpha_{\mathrm{out}} \hat{i}_v + \sin\alpha_{\mathrm{out}} \hat{i}_0 \tag{11}$$

the unit vector along the tether length. Here

$$\hat{i}_o = \hat{i}_r \times \hat{i}_v \tag{12}$$

is the unit vector perpendicular to the orbital plane, chosen in such a way that ($\hat{i}_r$, $\hat{i}_v$, $\hat{i}_o$) determines a right-handed orthogonal reference system. Furthermore we denoted with α_{in} and α_{out} the two angles which are necessary to define the tether position with respect to the vertical ($\hat{i}_r$). Here the in-plane angle α_{in} is the angle that the projection of the tether on the orbital plane makes with respect to $\hat{i}_r$ and the out-of-plane angle α_{out} gives, on the other hand, the deviation from the orbital plane.

Using (1), (4), (6) and (10), we obtain from eq. (9)

$$\mathrm{d}\Phi_{\mathrm{emf}} = -\, v_0 B_0 \, \mathrm{d}l [\cos\alpha_{\mathrm{in}} \cos\alpha_{\mathrm{out}} \cos\lambda + 2 \sin\alpha_{\mathrm{out}} \sin\theta \sin\lambda] \,. \tag{13}$$

In the approximation of small angles α_{in} and α_{out}, which will turn out to be well verified *a posteriori*, we have

$$\mathrm{d}\Phi_{\mathrm{emf}} = -\, v_0 B_0 \cos\lambda \, \mathrm{d}l \tag{14}$$

and the emf potential then depends on the orbital inclination only.

4. – Electrodynamic force and electrodynamic drag

The reaction of the current along the tether with the Earth's magnetic field induces a Lorentz force $\mathbf{F}_{\mathrm{e}}$ on the tether. The differential force on the element $\mathrm{d}l$ of the tether

is given by

$$\mathbf{dF}_{\mathrm{e}} = i(l)\, B_0(\hat{i}_l \times \mathbf{b})\, \mathrm{d}l\,.$$

The total force, which is obtained by integrating along the tether length, can be written as

$$\mathbf{F}_{\mathrm{e}} = B_0\, L\, I(\hat{i}_l \times \mathbf{b})\,, \tag{15}$$

where we define

$$I = \int_0^1 i(\xi)\, \mathrm{d}\xi \tag{16}$$

and, from now on, ξ will denote the dimensionless coordinate along the tether

$$\xi = \frac{l}{L}\,.$$

If we divide the force $\mathbf{F}_{\mathrm{e}}$ into its $\hat{i}_r$, $\hat{i}_v$ $\hat{i}_o$ components, we obtain, after some algebra,

$$\begin{aligned} F_{er} &= B_0\, L\, I[-\sin\alpha_{\mathrm{in}}\cos\alpha_{\mathrm{out}}\cos\lambda + \sin\alpha_{\mathrm{out}}\sin\lambda\cos\theta]\,,\\ F_{ev} &= B_0\, L\, I[\cos\alpha_{\mathrm{in}}\cos\alpha_{\mathrm{out}}\cos\lambda + 2\,\sin\alpha_{\mathrm{out}}\sin\lambda\sin\theta]\,,\\ F_{eo} &= -B_0\, L\, I\sin\lambda\cos\alpha_{\mathrm{out}}[\cos\alpha_{\mathrm{in}}\cos\theta + 2\sin\alpha_{\mathrm{in}}\sin\theta]\,. \end{aligned} \tag{17}$$

Notice that the out-of-plane electrodynamic force F_{eo} is proportional to $\sin\lambda$ and, therefore, it goes to zero for an orbit lying on the magnetic equator.

The electrodynamic force $\mathbf{F}_{\mathrm{e}}$ exerts a drag on the tether. The drag force F_{drag}, which is the one causing deorbiting of the spacecraft, is precisely given by the component of $\mathbf{F}_{\mathrm{e}}$ which is parallel to the velocity vector $\mathbf{v}$, *i.e.*,

$$F_{\mathrm{drag}} = \mathbf{F}_{\mathrm{e}}\cdot\hat{i}_v = F_{ev}, \tag{18}$$

with F_{ev} given in (17).

5. – Torque balance analysis

The equilibrium values of α_{in} and α_{out} are determined through a balance between the electrodynamic force, which tends to deviate the tether from the vertical direction, and the gravity gradient force which, on the contrary, tends to restore its vertical orientation. In this section we will derive the relevant equations for this balance.

We consider an orthogonal coordinate system whose axes (x, y, z) are aligned with the unit vectors ($\hat{i}_v$, $\hat{i}_o$, $\hat{i}_r$) previously defined, and whose origin is placed at the center of mass of the tethered system (see fig. 2). The gravity gradient force on a mass m_{b}, located at (x, y, z), is then given by [7]

$$\mathbf{F}_{\mathrm{g}} = F_{gr}\hat{i}_r + F_{go}\hat{i}_o \tag{19}$$

with

$$F_{gr} = 3m_{\mathrm{b}}\Omega^2 z\,, \qquad F_{go} = -m_{\mathrm{b}}\Omega^2 y \tag{20}$$

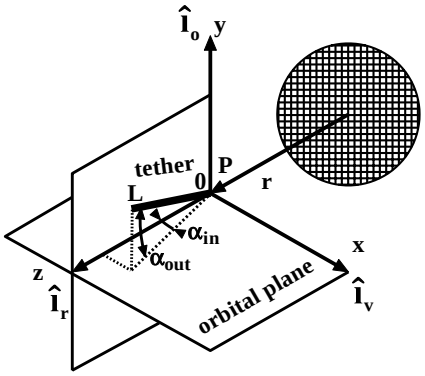

Fig. 2. – Orthogonal coordinate system associated with the tether.

Here

$$\Omega^2 = \frac{v_0^2}{r^2}$$

and m_b is the ballast mass, located at the upper tether termination. As the mass m_s of the satellite (at the lower termination), is much greater than m_b, the center of mass of the tethered system will essentially be at its lower end and, in terms of our angles α_{in} and α_{out}, the coordinates of m_b will be given by

$$(21) \qquad x = \mathbf{L}\cdot\hat{i}_v = L\cos\alpha_{out}\sin\alpha_{in}, \quad y = \mathbf{L}\cdot\hat{i}_o = L\sin\alpha_{out}, \quad z = \mathbf{L}\cdot\hat{i}_r = L\cos\alpha_{out}\cos\alpha_{in}.$$

From the definition

$$\mathbf{T}_g = \mathbf{L}\times\mathbf{F}_g = L(\hat{i}_l\times\mathbf{F}_g)$$

of the gravity gradient torque, we derive, using eq. (11) for $\hat{i}_l$ and (19) for $\mathbf{F}_g$:

$$(22) \quad \mathbf{T}_g = L\sin\alpha_{in}\cos\alpha_{out}[F_{go}\hat{i}_r - F_{gr}\hat{i}_o] + L[\sin\alpha_{out}F_{gr} - \cos\alpha_{in}\cos\alpha_{out}F_{go}]\,\hat{i}_v.$$

The in-plane rotations (*i.e.* the variations of α_{in}) are caused by the component of $\mathbf{T}_g$ perpendicular to the orbital plane, *i.e.*, using eqs. (20) and (21),

$$(23) \qquad T_g^{in} = \mathbf{T}_g\cdot\hat{i}_o = -3m_b\Omega^2L^2\cos^2\alpha_{out}\sin\alpha_{in}\cos\alpha_{in}.$$

On the other hand, rotations out of plane are caused by the projection of $\mathbf{T}_g$ on the orbital plane

$$\mathbf{T}_g^{(r,v)} = L\sin\alpha_{in}\cos\alpha_{out}F_{go}\hat{i}_r + L[\sin\alpha_{out}F_{gr} - \cos\alpha_{in}\cos\alpha_{out}F_{go}]\,\hat{i}_v.$$

The corresponding scalar torque, causing these variations, is found to be given by

$$(24) \qquad T_g^{out} = |\mathbf{T}_g^{(r,v)}| = m_b\Omega^2L^2\sin\alpha_{out}\cos\alpha_{out}(1+15\cos^2\alpha_{in})^{1/2}.$$

In the approximation of small angles α_{in} and α_{out}, we obtain for the torques associated to the gravity gradient

$$T_g^{in} = -3m_b\Omega^2 L^2\alpha_{in}, \quad T_g^{out} = 4m_b\Omega^2 L^2\alpha_{out}. \tag{25}$$

Finally, the tether mass m_t contributes to the gradient force and torque. As shown by Forward *et al.* [2], as far as the torque components are concerned, this contribution amount to the substitution of m_b with

$$m_{be} = m_b + \frac{m_t}{4}$$

in the previous formulas.

To calculate electrodynamic torques, we proceed in an entirely similar way. If we suppose the electrodynamic force to be uniformly distributed along the tether (a hypothesis which is well approximated only by the tether configurations including a balloon at the upper termination), then the electrodynamic force $\mathbf{F}_e$ can be considered as applied to the middle point of the tether and the electrodynamic torque is given by

$$\mathbf{T}_e = \frac{L}{2}(\hat{i}_l \times \mathbf{F}_e). \tag{26}$$

In terms of the components T_{er}, T_{ev}, T_{eo} of the torque $\mathbf{T}_e$ along the axes $\hat{i}_r$, $\hat{i}_v$ and $\hat{i}_o$, respectively, the magnitude of the torques acting on the in-plane and out-of-plane angles is given by

$$T_e^{in} = T_{eo}, \quad T_e^{out} = (T_{er}^2 + T_{ev}^2)^{1/2}. \tag{27}$$

We do not give here the complete expressions for these torques (derived from the definition (26) and eqs. (17) for the components of $\mathbf{F}_e$), but only the simplified formulas which are obtained in the small-angle approximation ($\alpha_{in} \ll 1$ and $\alpha_{out} \ll 1$). We have, to first order in α_{in} and α_{out},

$$T_{er} = -\frac{1}{2}B_0 L^2 I[\alpha_{in}\sin\lambda\cos\theta + \alpha_{out}\cos\lambda],$$

$$T_{ev} = \frac{1}{2}B_0 L^2 I\sin\lambda[\cos\theta + 2\alpha_{in}\sin\theta],$$

$$T_{eo} = \frac{1}{2}B_0 L^2 I[\cos\lambda + 2\alpha_{out}\sin\lambda\sin\theta].$$

Notice that, contrary to the torques associated to the gravity gradient, the components of the electrodynamic torque do depend on the orbital angle θ. However, at each point in the orbit, they are always counteracting the gravity gradient torques.

To lowest order in α_{in} and α_{out}, we obtain from the above formulas

$$T_e^{in} \sim \frac{1}{2}B_0 L^2 I\cos\lambda, \quad T_e^{out} \sim T_{ev} \sim \frac{1}{2}B_0 L^2 I\sin\lambda|\cos\theta|. \tag{28}$$

We see that the out-of-plane torque vanishes for an orbit lying on the magnetic equator. Consequently, for such an orbit, the tether deviates from the vertical but remains in the plane of the orbit. As for the variation of the torque T_e^{out} with θ, as in the following treatment (see sect. **7**) we will refer to day-night averages of the ionospheric density, we will, correspondingly, consider the average of T_e^{out} over one orbital period which is then given by

$$T_e^{out} \sim \frac{1}{\pi} B_0 L^2 I \sin\lambda .$$

With that, balancing now gravity gradient and electrodynamic torques, we obtain for the angles α_{in} and α_{out},

$$\alpha_{in} \sim \frac{1}{6} \frac{B_0 I}{m_{be}\Omega^2} \cos\lambda , \qquad \alpha_{out} \sim \frac{1}{4\pi} \frac{B_0 I}{m_{be}\Omega^2} \sin\lambda , \tag{29}$$

so that $\alpha_{out}/\alpha_{in} \sim 0.5 \ \mathrm{tg}\,\lambda$. Notice that eqs. (29) are not to be viewed as solutions for the equilibrium values of α_{in} and α_{out} as the current I, on the right-hand sides, will also in general depend on these angles.

6. – Analysis of the tether electrical circuit

We provide in this section the analysis of the tether electrical circuit leading to the determination of the current I which is needed for the evaluation of the drag force F_{drag} and of the components of the angles α_{in} and α_{out} through eqs. (29). As we will see, the problem is a simple generalization of the one solved for equatorial orbits and a vertical tether in the study of ref. [6], so that we will be able to use the formulas obtained in that study. We will provide results for both the BTB and the ITB configurations.

6˙1. *Current and potentials along the tether.* – Referring to the BTB configuration and using the OML approximation [8], we have for the current along the tether

$$i(\xi) = i_0 \int_{\xi}^{1} \mathrm{d}\xi' [1 + \tilde{\Phi}(\xi')]^{1/2} + i_b, \tag{30}$$

where

$$i_0 = 2\pi r_w L j_0$$

is the thermal current collected by the tether ($j_0 = e n_0 v_{the}/4$ being the thermal current density) and i_b is the current collected by the balloon which is at potential $\Phi_b = \Phi(\xi = 1)$. In (30), and in the following, we use $\tilde{\Phi} = e\Phi/kT_e$. Finally, the balloon current i_b is given, in terms of the balloon potential Φ_b, by

$$i_b = 1.56 \times 10^{-15} r_b^2 n_0 T_e^{0.5} + 1.79 \times 10^{-11} r_b^{1.37} n_0^{0.685} T_e^{0.343} \Phi_b^{0.472}, \tag{31}$$

which we derive by scaling TSS-1R data [9]. In eq. (31) r_b is in m, n in m^{-3} and T_e in K.

For the ITB configuration, it is simply

$$i(\xi) = i_b .$$

For the variation of voltage Φ (not only emf voltage) along the tether we have to add to (13) the effect of ohmic losses and obtain

$$\mathrm{d}\Phi = \mathrm{d}\Phi_{\mathrm{emf}} - i(l)\,\mathrm{d}R\,, \tag{32}$$

where $i(l)$ is the current flowing through the tether element between l and $l + \mathrm{d}l$ and

$$\mathrm{d}R = \frac{R_{\mathrm{t}}}{L}\,\mathrm{d}l$$

is the resistance of that element, with R_{t} the total tether resistance. We will use $R_{\mathrm{t}} = 280\ \Omega$ which refers to an Al tether (with a conductive oxidation-resistant coating), of length $L = 5$ km and radius $r_w = 0.4$ mm. The differential problem (32) for the variation of the voltage Φ along the tether length was solved in ref. [6] for the simplest case of an equatorial orbit and assuming a vertically oriented straight tether. In that case, we used, for the differential of the emf potential,

$$\mathrm{d}\Phi_0 = V_0 B_{\mathrm{e}}\,\mathrm{d}l$$

with $B_{\mathrm{e}} = 0.3$ G and the orbital velocity assumed to be constant at the value $V_0 = 7.5$ km/s. Comparing with (13), we see that, in the more general case we want to treat now, we can write

$$\mathrm{d}\Phi_{\mathrm{emf}} = f\,\mathrm{d}\Phi_0$$

with

$$f = \frac{1.054}{\tilde{r}^{7/2}}\left[\cos\alpha_{\mathrm{in}}\cos\alpha_{\mathrm{out}}\cos\lambda + 2\,\sin\alpha_{\mathrm{out}}\sin\theta\sin\lambda\right] \tag{33}$$

and

$$\tilde{r} = \frac{r}{R_{\mathrm{e}}}\,.$$

From (32) we then obtain

$$\frac{\mathrm{d}\Phi}{\mathrm{d}\xi} = \Phi_0 f\left(1 - \frac{i(\xi)}{i_m}\right), \tag{34}$$

with

$$\Phi_0 = V_0 B_{\mathrm{e}} L\,, \qquad i_m = f i_{m0}$$

and

$$i_{m0} = \frac{\Phi_0}{R_{\mathrm{t}}}\,.$$

Differentiating eq. (34), using (30), we obtain

$$\frac{\mathrm{d}^2 \Phi}{\mathrm{d}\xi^2} = \Phi_0 \frac{i_0}{i_{m0}} (1 + \widetilde{\Phi})^{1/2}$$

with boundary conditions

$$\Phi(\xi = 0) = 0 , \qquad i(\xi = 1) = i_\mathrm{b}$$

the second of which gives

$$\frac{\mathrm{d}\Phi}{\mathrm{d}\xi} = f\Phi_0 \left(1 - \frac{i_\mathrm{b}}{i_m}\right).$$

Introducing, in place of the potential Φ, the variable

$$y = \frac{1 + \widetilde{\Phi}}{\widetilde{\Phi}_0} \tag{35}$$

as in the previous treatment [6], we obtain for y the equation

$$\frac{\mathrm{d}^2 y}{\mathrm{d}\xi^2} = \frac{i_0}{i_{m0}} \widetilde{\Phi}_0^{1/2} y^{1/2} \tag{36}$$

with boundary conditions

$$y(\xi = 0) = y_0 \equiv \frac{1}{\widetilde{\Phi}_0} , \qquad \frac{\mathrm{d}y}{\mathrm{d}\xi}(\xi = 1) = f\left(1 - \frac{i_\mathrm{b}}{i_m}\right). \tag{37}$$

Integrating once eq. (36), using the second of the boundary conditions (37), we end up with

$$\left(\frac{\mathrm{d}y}{\mathrm{d}\xi}\right)^2 = H + Ay^{3/2} \tag{38}$$

with

$$A = \frac{4}{3} \frac{i_0}{i_{m0}} \widetilde{\Phi}_0^{1/2}, \qquad H = f^2 \left(1 - \frac{i_\mathrm{b}}{i_m}\right)^2 - Ay_\mathrm{b}^{3/2}. \tag{39}$$

Equation (38) is the same equation used in the previous study [6]. The only difference is in the definition of the quantities A, H and i_m which now contain the scale factor f defined in eq. (33). Therefore, from here on, all the formalism developed applies with no change. In the following we will summarize just what we need to arrive at the calculation of the drag force.

For the ITB configuration, on the other hand, the equation for y is simply

$$\frac{\mathrm{d}y}{\mathrm{d}\xi} = f - \frac{i_\mathrm{b}}{i_{m0}}$$

which, together with the boundary condition $y(\xi = 0) = y_0$, gives

$$y = \left(f - \frac{i_b}{i_{m0}} \right) \xi + y_0 . \tag{40}$$

6˙2. *Equations for the potential Φ_b of the upper tether termination.* – Referring first to the BTB configuration, the equations to be used for the potential at the upper termination $y_b = y(\xi = 1)$ vary according to the value of a certain parameter ξ^* which can be evaluated only after the solution y_b has been found. This parameter is defined by

$$\xi^* = \frac{1}{\sqrt{H}} (y^* - y_0)$$

with

$$y^* = \left(\frac{H}{A} \right)^{2/3} .$$

To obtain y_b, we have to solve the following equations:

$$y_b = \left[\frac{1}{4} \sqrt{A} (1 - \xi^*) + y^{*1/4} \right]^4 , \quad \text{if } \xi^* < 1 , \tag{41}$$

$$y_b = \sqrt{H} + y_0 , \quad \text{if } \xi^* > 1 . \tag{42}$$

For the ITB configuration, from eq. (40), we obtain for y_b the equation

$$y_b = f - \frac{i_b}{i_{m0}} + y_0 . \tag{43}$$

6˙3. *Formulas for the current I.* – To calculate the drag force, given by eq. (18), we need the integral I of the current along the tether for which we just recall the formulas already derived in ref. [6]. We have, for the BTB configuration,

$$I = [i_0 \tilde{\Phi}_0^{1/2} Y + i_b] \tag{44}$$

with

$$Y = \frac{2}{3} \frac{1}{\sqrt{H}} \left[\xi^* (\sqrt{H} \xi^* + y_0)^{3/2} - \frac{2}{5} \frac{1}{\sqrt{H}} [(\sqrt{H} \xi^* + y_0)^{5/2} - y_0^{5/2}] \right] + \tag{45}$$

$$+ \frac{4}{3} \frac{1}{\sqrt{A}} \xi^* (y_b^{3/4} - y^{*3/4}) + \frac{4}{3} \frac{1}{\sqrt{A}} \left[y_b^{3/4} (1 - \xi^*) - \frac{1}{\sqrt{A}} (y_b - y^*) \right], \quad \text{for } \xi^* < 1$$

and

$$Y = \frac{2}{3} \frac{1}{\sqrt{H}} \left[y_b^{3/2} - \frac{2}{5} \frac{1}{\sqrt{H}} (y_b^{5/2} - y_0^{5/2}) \right], \quad \text{for } \xi^* > 1 . \tag{46}$$

The various quantities appearing in these equations have been defined in subsects. **6**˙1 and **6**˙2.

For the ITB configuration, on the other hand, we have simply

$$I = i_b . \tag{47}$$

Notice now that the current I depends on the angles α_{in} and α_{out} (and the orbital angle θ) only through the emf potential (13) or, equivalently, the scale factor f given by eq. (33). However, as seen from eq. (14), in the small-angles approximation, the emf potential does not depend on the above angles anymore. This means that, to zeroth order in α_{in} and α_{out}, the current is independent of α_{in} and α_{out} and, in turn, this implies that eqs. (29) become explicit solutions for α_{in} and α_{out}. The small-angle approximation will have of course to be verified once the current and, therefore, the angles α_{in} and α_{out} are obtained.

7. – Satellite decay

Let us first discuss the ionospheric model that we used in our calculations of orbital decay due to electrodynamic drag. Variations of electron temperature in the ionosphere are quite small and, on the other hand, the dependence on temperature, in our formulas (see eq. (31)), is rather weak. For this reason, we have used everywhere a constant temperature $T_e = 2000$ K. The variation of density with altitude which has been assumed (in the range 1500–200 km) is shown in fig. 3. It has been derived from Hanson (1965) [10] and corresponds to medium sunspot conditions and an average between day and night values or, equivalently, an average value for each orbit. We will show that referring to a more sophisticated ionospheric model (the IRI model) does not alter the results.

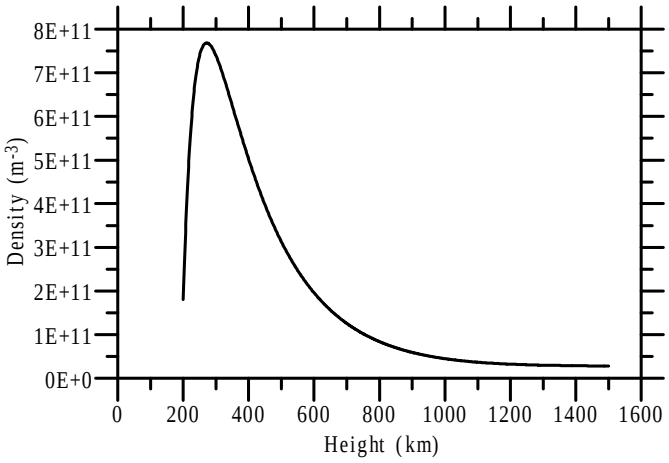

Fig. 3. – Profile of ionospheric density *vs.* altitude (data obtained from ref. [10]).

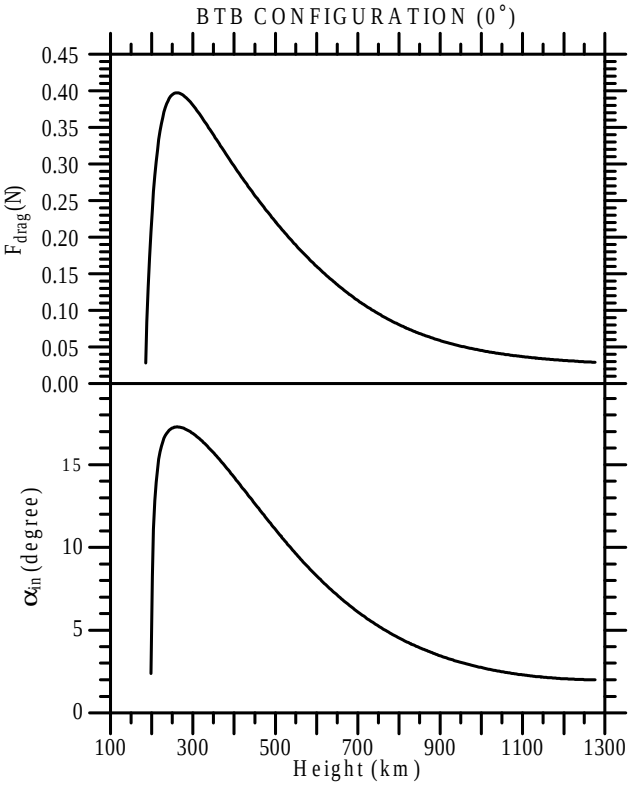

Fig. 4. – Altitude profiles of electrodynamic drag (upper panel) and the angle α_{in} of deviation of the tether with respect to the vertical (lower panel) for an equatorial orbit and the BTB configuration.

The time T needed to deorbit a satellite between two given heights (corresponding to orbital radii a_1 and a_2 with $a_1 < a_2$) is given by

$$\Delta t = \frac{1}{2}\int_{a_1}^{a_2} \frac{GM_{\text{e}} m_{\text{s}}}{a^2 F_{\text{drag}} v_0}\,\text{d}a\,, \tag{48}$$

where m_{s} is the total mass of the deorbiting system (satellite mass + mass of the tether system).

In this section we present several results obtained with the formalism previously developed. We always refer to a tether length $L = 5$ km, a tether radius $r_{\text{w}} = 0.4$ mm and a balloon radius $r_{\text{b}} = 2.5$ m. Furthermore, unless specified otherwise, we will refer to a 500 kg satellite, a ballast mass of 30 kg and a tether mass of 7 kg.

Figure 4 shows the altitude profiles of the electrodynamic drag and the angle α_{in} of deviation from the vertical obtained for an equatorial orbit and the BTB configuration. As already remarked, it is $\alpha_{\text{out}} = 0$ for equatorial orbits. The profiles of fig. 4 follow, obviously, the density profile of fig. 3. Notice that the maximum value of α_{in}, obtained in correspondence to maximum density, is $\sim 17°$. Smaller values of α_{in} are obtained, as

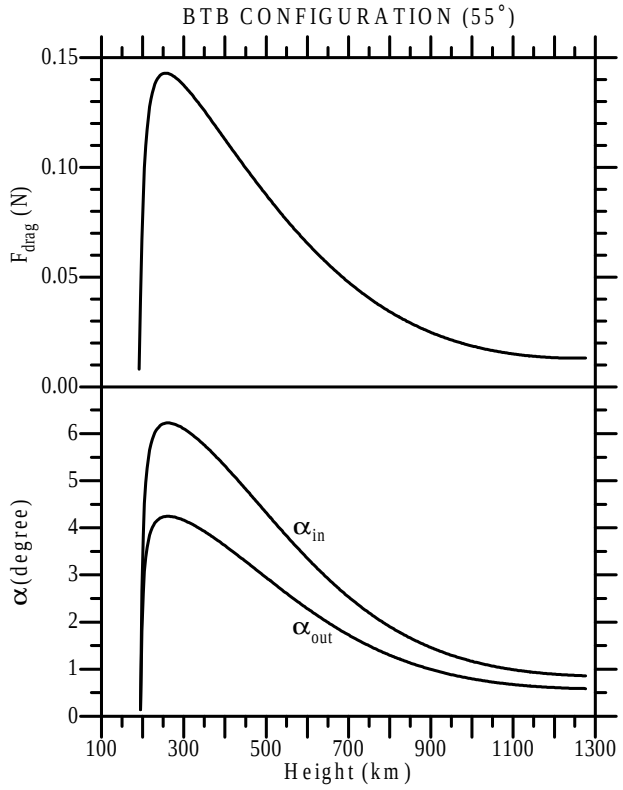

Fig. 5. – Altitude profiles of electrodynamic drag (upper panel) and the angles α_{in} and α_{out} of deviation of the tether with respect to the vertical (lower panel) for an orbit at 55° inclination and the BTB configuration.

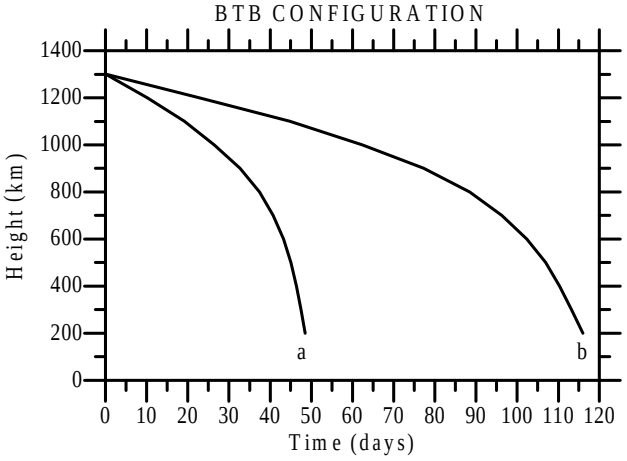

Fig. 6. – Decay profiles for the BTB configuration: a) equatorial orbit; b) 55° orbit.

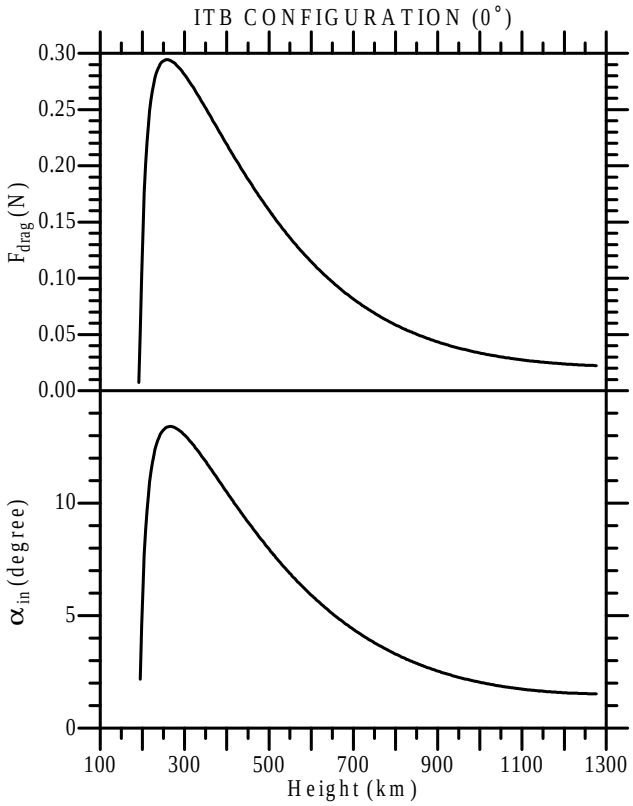

Fig. 7. – Altitude profiles of electrodynamic drag (upper panel) and the angle α_{in} of deviation of the tether with respect to the vertical (lower panel) for an equatorial orbit and the ITB configuration.

will be seen, for inclined orbits. This is shown in fig. 5 which refers to an orbit at 55° inclination. The upper panel in the figure is the profile of the drag force and, in the lower panel, we have plotted both angles α_{in} and α_{out}. The maximum value of α_{in} is now at $\sim 6°$ and α_{out} is always smaller. We see therefore that a small-angle approximation (for α_{in} and α_{out}), is *a posteriori* justified (also for equatorial orbits).

Figure 6 gives the profiles of orbital decay obtained for the equatorial and the 55° orbit, still for the BTB configuration. To descend from 1300 to 200 km, we go from ~ 48 days for the equatorial orbit to ~ 116 days for the orbit at 55°. Notice that the value obtained for the equatorial orbit ($\sim$ 48 days), is longer than that (~ 23 days) obtained in the previous simplified calculation [6] where variations of v_0 and B_0 with altitude were neglected and the tether was assumed to be vertical.

The same results with an insulated tether (configuration ITB) are shown in figs. 7, 8 and 9. Notice that, at least for the tether and balloon dimensions considered, the BTB configuration performs better than the ITB configuration. The total decay time, in passing from the BTB to the ITB configuration, increases from 48 days to ~ 65 days for the case of the equatorial orbit, and, from 116 days to 150 days for the 55° orbit. Thus the results of the comparison analyzed in ref. [6] are confirmed by these more realistic

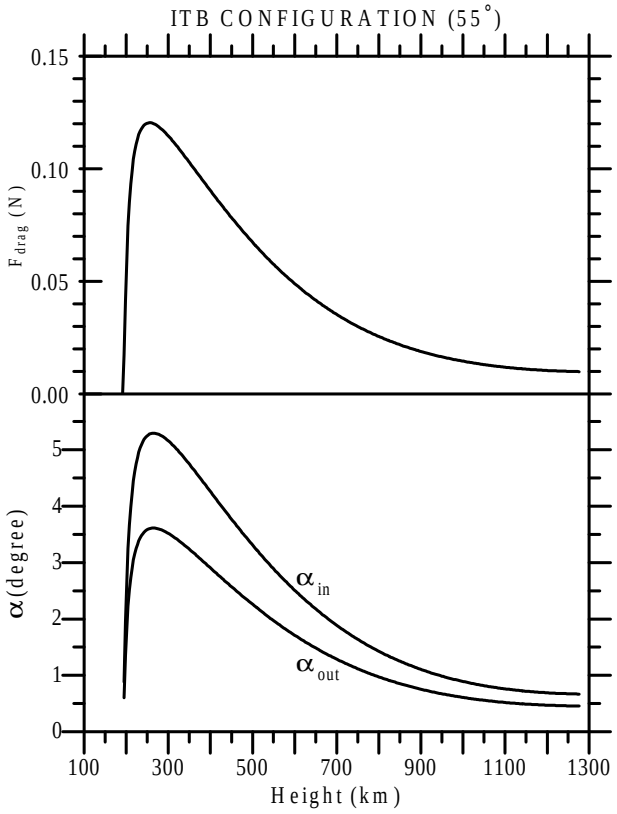

Fig. 8. – Altitude profiles of electrodynamic drag (upper panel) and the angle α_{in} and α_{out} of deviation of the tether with respect to the vertical (lower panel) for an orbit at 55° inclination and the ITB configuration.

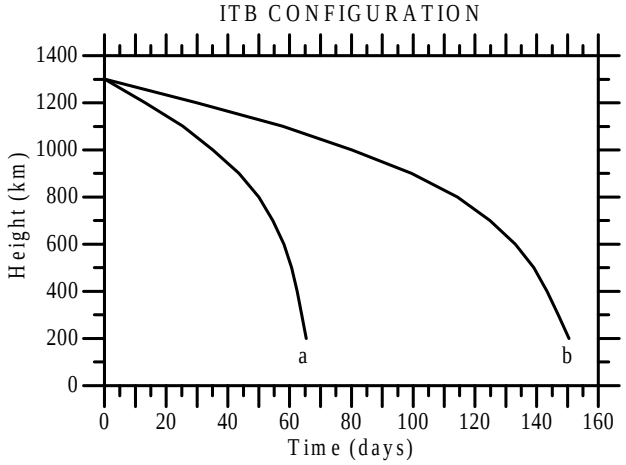

Fig. 9. – Decay profiles for the ITB configuration: a) equatorial orbit; b) 55° orbit.

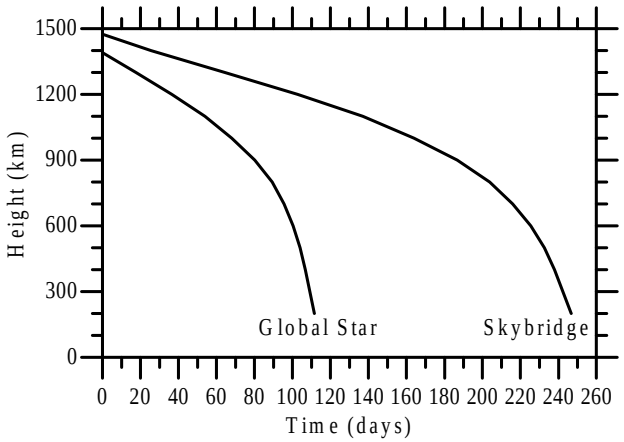

Fig. 10. – Decay profiles for Global Star and Skybridge satellites using a BTB configuration.

calculations. Notice also that, for a total mass of the satellite (including the tether system) of 500 kg (the value used in ref. [10]), the decay time for the 55° inclination orbit and the ITB configuration becomes ∼150 days and, therefore, agrees very well with the number calculated in ref. [11] (∼140 days), for the same configuration, using an IRI ionospheric model. This means that our assumption of a constant temperature (of 2000 K) and the orbital averages of various quantities (first of all the ionospheric density) used here are adequate and, in computing deorbiting, we do not need to increase further the complexity of the ionospheric model.

Finally, we want to apply our formalism to the calculation of deorbiting of some specific constellation of satellites. We chose Global Star (mass = 450 kg, altitude = 1390 km, orbital inclination = 52°) and Skybridge (mass = 800 kg, altitude = 1475 km, orbital inclination = 55°). The decay profiles down to 200 km and with a BTB configuration for satellites of these two constellations are shown in fig. 10. The total deorbiting time turns out to be ∼111 days for Global Star and ∼247 days for Skybridge. For the same constellation satellites, Forward *et al.* [2], in a calculation essentially ignoring the real tether electrical circuit, gave 37 and 46 days, respectively. We have commented elsewhere [6] that it had to be expected these numbers to be unrealistically short. On the other hand, we believe that the values obtained here are quite realistic in that the tether electrodynamic interaction with the ionosphere has been accurately considered.

8. – Conclusions and discussion

We have provided realistic calculations of the time needed to deorbit a LEO satellite with the use of a conducting tether. The calculation takes fully into account the tether equivalent electric circuit resulting from the interaction with the ionospheric medium and has been done with reference to a dipole model for the Earth's magnetic field and a model for the altitude variation of electron density.

On the basis of a previous comparative study [6] between different tether systems, showing the advantage of using a conducting balloon to collect electrons at the upper

tether termination, we have provided results for the two configurations (BTB and ITB) including such a conducting balloon, either with a bare tether, or with a conducting insulated tether. We recall that, as discussed in ref. [6], the use of an upper balloon, besides improving the performance of the system, makes the distribution of the drag force along the tether more uniform, which might be a relevant point for the dynamical stability of the system.

An important point of the study is that the angles α_{in} and α_{out} of deviation of the tether from the vertical position, due to the balance between gravity gradient and electrodynamic torques, have been calculated and taken into account. As is well known, these angles are of importance for the dynamical stability of the system and, although critical values for instability onset are not known, it would be good practice to maintain them small during the deorbitation of the given object.

Referring to specific tether and balloon dimensions ($L = 5$ km, $r_{\text{w}} = 0.4$ mm, $r_{\text{b}} = 2.5$ m), we can calculate deorbiting times for different orbital inclinations. We have given results for equatorial orbits and for orbits at 55° inclination (this value being typical for several constellation satellites). In addition, the formalism has been applied to two specific constellation satellites (Global Star and Skybridge).

We found a total time to deorbit from 1300 to 200 km, of $\sim$ 116 days for the 55° orbit and a 500 kg satellite, and times considerably shorter for equatorial orbits. With these results, the product decay time–cross-section of the tethered deorbiting system is enormously smaller than the equivalent product for the satellite only (*i.e.* using its natural decay time).

As for the in-plane angle α_{in} of deviation of the tether from the vertical direction, we found a maximum value of the angle α_{in} of $\sim 20°$, in correspondence to the density maximum (at $\sim$ 300 km), during decay of an equatorial orbit. On the other hand, when we refer to the 55° inclined orbit (typical of many constellation satellites), the angle α_{in} is much smaller (maximum of $\sim 6°$) and the out-of-plane angle α_{out} even smaller.

Our results refer of course to specific tether and balloon dimensions and we have not attempted here a parametric study directed to optimize the system dimensions with respect to a given criterium (for example, an upper value of the deorbiting time required for tether survivability). Although this is left to a future study, we point out here that, increasing the length of the tether and/or the radius of the balloon, would obviously increase the electrodynamic drag and, therefore, lead to larger values of the angles α_{in} and α_{out} which might be unacceptable for the stability of the system. With the dimensions chosen, the tether system to be attached to the satellite is indeed quite simple and, on the other hand, both the decay times obtained and the variations of the angles α_{in} and α_{out} appear to be acceptable.

In conclusion, it appears to be confirmed, from a realistic calculation, that the use of electrodynamic tethers is an extremely simple and effective way of curing, at least in part, the debris problem.

REFERENCES

[1] ANSELMO L., ROSSI A. and PARDINI C., *Updated results of the long term evolution of the space debris environment, Adv. Space Res.*, **23** (1999) 201-211.

[2] FORWARD R L., HOYT R. P. and UPHOFF C., *Application of the Terminator Tether electrodynamic drag technology to the de-orbit of constellation spacecraft, 34th Joint Propulsion Conference, Cleveland, OH, July 1998*, AIAA Paper 98-3491.

[3] JOHNSON L. and BALLANCE J., *Propulsive Small Expendable Deployer System* (*ProSEDS*) *Space Demonstration* in *Tether Technology Interchange Meeting*, NASA/CP-1998-206900 (1998) p. 103.
[4] ANSELMO L. and PARDINI C., *Assessing the impact risk of orbital debris on space tethers*, to be published in *Space Debris*, 2000.
[5] HOYT R. P. and FORWARD R. L., *The Hoytether: A Failsafe Multiline Space Tether Structure*, in *Tether Technology Interchange Meeting*, NASA/CP - 1998-206900 (1998) p. 369.
[6] VANNARONI G., DOBROWOLNY M. and DE VENUTO F., *The use of electrodynamic tethers to de-orbit LEO spacecraft*, Istituto Fisica Spazio Interplanetario, Rome, IFSI-99-6, 1999.
[7] ARNOLD D. A., *Tether Tutorial, Proceedings of Space Tethers for Science in the Space Station Era, Venice 4-8 October 1987*, edited by L. GUERRIERO and I. BEKEY, *SIF Conf. Proc.*, Vol. **14** (Editrice Compositori, Bologna) 1987, pp. 26-36.
[8] SCHOTT L., *Electrical probes*, in *Plasma diagnostics*, edited by W. LOCHTE-HOLTGREVEN (North-Holland Publishing Company, Amsterdam) 1968.
[9] DOBROWOLNY M., VANNARONI G. and DE VENUTO F., *Electron collection by a charged satellite in the ionospheric plasma*, *Nuovo Cimento C*, **22** (1999) 207.
[10] HANSON W. B., *Structure of the ionosphere*, in *Satellite Environment Handbook*, edited by F. S. JOHNSON (Stanford University Press, Stanford, CA) 1965.
[11] IESS L., BRUNO C., ULIVIERI C. and VANNARONI G., *Satellite de-orbiting by means of electrodynamic tethers: System Configuration and Performance*, *49th International Astronautical Congress, September 28-October 2 1998, Melbourne, Australia*, IAF-98-S.606.